distance is represented in Fig. 5 (dots), together with the theoretical curve (solid line), calculated from Eq. (27). It can be observed that, at the exit of the DWD, the measured DOP is nearly zero, but it grows as the light propagates and reaches a maximum value, near unity, for a propagation distance around 2.75 m. Around this distance, the light is nearly totally polarized. Then, the DOP decreases to nearly zero when the propagation distance is around 5.5 m. This behavior is periodically repeated with increasing propagation distance. A complete agreement between calculated curve and experimental points is obtained.

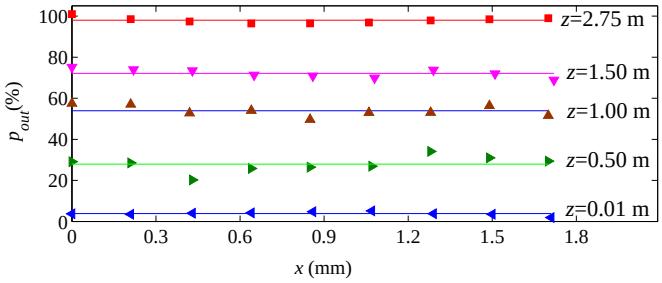

Fig. 4. Measured values of the DOP as a function of transverse displacement for several planes after the DWD when an unpolarized plane wave impinges on the DWD.

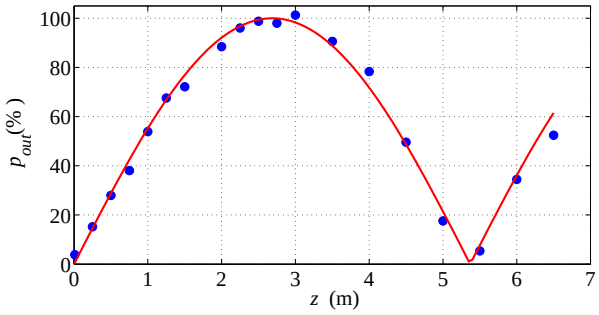

Fig. 5. Experimental and theoretical DOP as a function of the free space propagation distance after the DWD when an unpolarized plane wave impinges on the DWD.

Figure 6 shows the measured $s_1(x,z)$, $s_2(x,z)$ and $s_3(x,z)$ Stokes parameters (normalized to the total intensity I_0) at transverse planes located at different z distances behind the DWD (red circles: s_1; green down triangles: s_2; blue up triangles: s_3). At $z = 0.01$ m, the all three Stokes parameters are approximately zero, representing unpolarized light. For $z = 0.50$ m, the Stokes parameters $s_1(x,z)$ and $s_3(x,z)$ follow sinusoidal dependences *vs* the transverse variable x (with 0.28 maximum amplitude and a quarter-period delay), while $s_2(x,z) \approx 0$. Similar results are observed for $z = 1.50$ m and $z = 2.75$ m but with larger maximum amplitude (0.72 and 0.97, respectively) than in the previous case. Theoretical curves obtained by means of Eq. (26) are also represented for these distances. A very good agreement with experimental data is observed.

4. Conclusions

DWD's are optical devices used when a reduction of the DOP of light is required. Being deterministic objects, they are actually *pseudo-depolarizers* and their effect is to produce a periodic

#177860 - $15.00 USD Received 10 Oct 2012; accepted 1 Nov 2012; published 20 Nov 2012

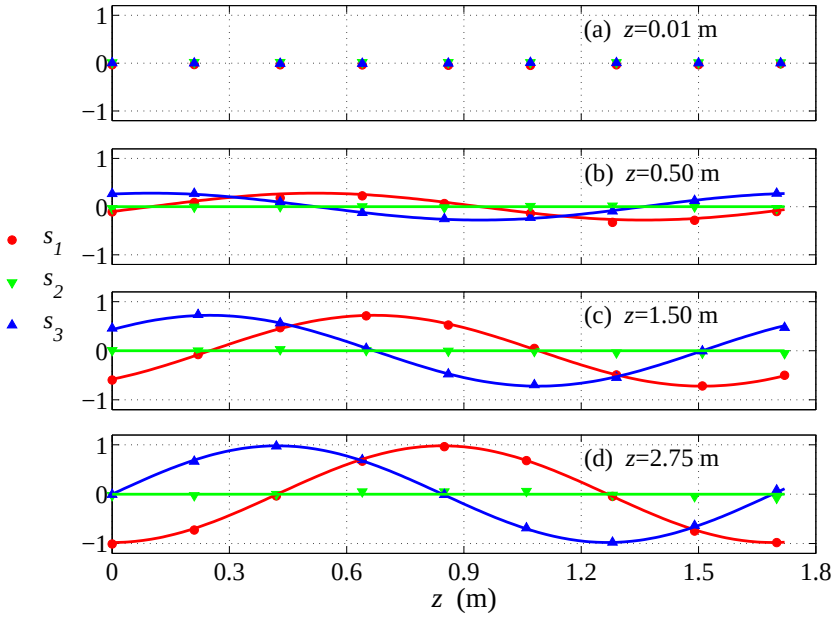

Fig. 6. Measured Stokes parameters (symbols) of the exiting light at several z-planes when an unpolarized plane wave impinges on the DWD. Calculated values (solid lines) are also represented at $z = 0.50$, $z = 1.50$, m and at $z = 2.75$ m. All values are normalized to the input intensity I_0.

transverse variation of the polarization state of the field at their output, as the one produced by a polarization grating. As a consequence, the DOP of the output field, evaluated averaging the Stokes parameters over a sufficiently large area, turns out to be nearly zero.

In this paper, the polarization characteristics of the field produced when an unpolarized plane wave passes through a DWD have been analyzed. One of the obtained results is that, although the output field presents a periodic variation of its polarization state, the (local) DOP is uniform across any transverse plane. Furthermore, the DOP at the exit face of the DWD is zero, but it changes periodically on increasing the distance from the device. In particular, it becomes unitary at a distance corresponding to a quarter of the Talbot distance pertaining to the period of the polarization pattern produced by the DWD. The origin of such behavior arises from the superposition of two mutually uncorrelated transversally periodic polarization patterns. An experiment has been carried out to confirm the theoretical predictions.

The above properties of the DOP are exactly expected when the incident field is an ideal plane wave, and without any transverse limitations of the device. In a real experiment, the oscillating behavior of the DOP is expected only within a finite range of distances, corresponding to the region where the different fields emerging from the device overlap. Nonetheless, such a range is of the order of some tens of meters long for a typical DWD, so that several periods of the DOP oscillation can be observed.

Finally it should be noted that DWD's could be used for generating periodic polarization structures, whose DOP can be varied at will, on changing the propagation distance beyond the device.

#177860 - $15.00 USD Received 10 Oct 2012; accepted 1 Nov 2012; published 20 Nov 2012

Appendix

In this appendix, the expressions of the fields at the exit of the DWD are derived. Three-dimensional fields with generally nonvanishing z components are considered, so that the field of a plane wave, linearly polarized along x, normally incident on the DWD can be written as

$$\mathbf{E}_{in}^{(x)}(x_i,-d) = A\begin{pmatrix}1\\0\\0\end{pmatrix}, \tag{30}$$

where A is its amplitude and x_i is the x-coordinate across the entrance surface of the device.

The phase of the field at a typical point $(x, z>0)$ at the exit of the DWD is obtained by evaluating the optical path length along the line sketched in Fig. 1(b), which represents a flux line of the wave vector inside the crystal. The amplitude of the field is derived using the transmission coefficients pertinent to every interface along the optical path.

From simple geometrical considerations, the following relation can be derived between the transverse coordinate of the optical path beyond the device and the corresponding one at its entrance surface:

$$x_i = \frac{x - z\tan\gamma_{oe} - d_2\tan\beta_{oe}}{1-\tan\alpha\,\tan\beta_{oe}}. \tag{31}$$

After propagating along the distance $(d_1 + x_i\tan\ \alpha)$ inside the first wedge as an ordinary wave, the field becomes

$$\mathbf{E}_{xo}^{(x)}(x_i,-d_2+x_i\tan\alpha) = A\,t_{xo}\begin{pmatrix}1\\0\\0\end{pmatrix}\exp\left[-ik_o\left(d_1+x_i\tan\alpha\right)\right]. \tag{32}$$

At the interface between the two crystals, this wave splits into an ordinary wave (*oo*) and an extraordinary wave (*oe*). The corresponding Snell's laws are

$$k_o\sin\alpha = k_o\sin\left(\beta_{oo}+\alpha\right), \tag{33}$$

$$k_o\sin\alpha = k_{oe}\sin\left(\beta_{oe}+\alpha\right). \tag{34}$$

The *oo* wave propagates along the z axis up to the exit surface of the device, where the field turns out to be

$$\mathbf{E}_{oo}^{(x)}(x_i,z=0^-) = A\,t_{xo}t_{oo}\begin{pmatrix}\cos(\pi/4)\\-\sin(\pi/4)\\0\end{pmatrix}\exp\left(-ik_od\right), \tag{35}$$

and after the exit surface it becomes

$$\mathbf{E}_{oo}^{(x)}(x,z>0) = \frac{A}{\sqrt{2}}\,t_{xo}t_{oo}\begin{pmatrix}t_{ox}^{(x)}\\-t_{oy}^{(x)}\\0\end{pmatrix}\exp\left(-ik_od-ikz\right). \tag{36}$$

On the other hand, the *oe* field across the inner side of the exit DWD face is [29, 30]

$$\mathbf{E}_{oe}^{(x)}(x_{oe},z=0^-) = A\,t_{xo}t_{oe}\begin{pmatrix}e_{oe,x}\\e_{oe,y}\\e_{oe,z}\end{pmatrix}\exp\left[-ik_o\left(d_1+x_i\tan\alpha\right)-ik_{oe}\frac{\left(d_2-x_i\tan\alpha\right)}{\cos\beta_{oe}}\right], \tag{37}$$

where $x_{oe} = d_2\tan\beta_{oe} + x_i\left(1-\tan\alpha\tan\beta_{oe}\right)$ and $(e_{oe,x}, e_{oe,y}, e_{oe,z})^T$ (with the superscript T denoting transpose) is a unitary vector perpendicular to the *oe* ray vector that lies in the plane

#177860 - $15.00 USD Received 10 Oct 2012; accepted 1 Nov 2012; published 20 Nov 2012

formed by the second crystal optic axis and the wave vector of the *oe* wave. The angle β_{oe} is obtained from Eqs. (9) and (34), taking into account that $\cos\varphi_{oe} = \frac{1}{\sqrt{2}}\sin\beta_{oe}$ (see the optic axis orientation in Fig. 1(a)). Finally, the *oe* field propagating beyond the DWD turns out to be

$$\begin{aligned} \mathbf{E}_{oe}^{(x)}(x, z>0) &= \frac{A}{\sqrt{2}}\, t_{xo} t_{oe} \begin{pmatrix} t_{ex}^{(x)} \cos\gamma_{oe} \\ t_{ey}^{(x)} \\ t_{ex}^{(x)} \sin\gamma_{oe} \end{pmatrix} \\ &\times \exp\left[-ik_o\left(d_1 + x_i \tan\alpha\right) - \frac{ik_{oe}\left(d_2 - x_i\tan\alpha\right)}{\cos\beta_{oe}} - \frac{ikz}{\cos\gamma_{oe}} \right], \end{aligned} \tag{38}$$

where the refraction angle γ_{oe} is obtained on applying the Snell's law at the exit surface. On replacing the x_i value given in Eq. (31), the latter equation becomes

$$\begin{aligned} \mathbf{E}_{oe}^{(x)}(x, z>0) &= \frac{A}{\sqrt{2}}\, t_{xo} t_{oe} \begin{pmatrix} t_{ex}^{(x)} \cos\gamma_{oe} \\ t_{ey}^{(x)} \\ t_{ex}^{(x)} \sin\gamma_{oe} \end{pmatrix} \\ &\times \exp\left(-ik_o d_1 - id_2 k_{oe}\cos\beta_{oe} - ixk\sin\gamma_{oe} - izk\cos\gamma_{oe}\right). \end{aligned} \tag{39}$$

If the z component of the above field is neglected, the superposition of the *oo* and *oe* waves in Eqs. (36) and (39) gives the field in Eq. (6).

Following an analogous procedure, but with an incident plane wave linearly polarized along y, it is found that

$$\begin{aligned} \mathbf{E}_{eo}^{(y)}(x, z>0) &= \frac{A}{\sqrt{2}}\, t_{ye} t_{eo} \begin{pmatrix} -t_{ox}^{(y)} \cos\gamma_{eo} \\ t_{oy}^{(y)} \\ -t_{ox}^{(y)} \sin\gamma_{eo} \end{pmatrix} \\ &\times \exp\left(-ik_e d_1 - ik_o d_2\cos\beta_{eo} - ikx\sin\gamma_{eo} - ikz\cos\gamma_{eo}\right), \end{aligned} \tag{40}$$

as the output field for the *eo* wave, and

$$\begin{aligned} \mathbf{E}_{ee}^{(y)}(x, z>0) &= \frac{A}{\sqrt{2}}\, t_{ye} t_{ee} \begin{pmatrix} t_{ex}^{(y)} \cos\gamma_{ee} \\ t_{ey}^{(y)} \\ t_{ex}^{(y)} \sin\gamma_{ee} \end{pmatrix} \\ &\times \exp\left(-ik_e d_1 - ik_{ee} d_2\cos\beta_{ee} - ikx\sin\gamma_{ee} - ikz\cos\gamma_{ee}\right), \end{aligned} \tag{41}$$

for the *ee* wave. Again, on assuming as negligible the z components of such fields, their superposition gives rise to the field expressed in Eq. (13).

Acknowledgments

One of the authors (J. C. G. S.) is grateful to a grant from 2011 Fundación Caja Madrid Program. J. C. G. S. and G. P. acknowledge the hospitality of Prof. F. Gori's group.

#177860 - $15.00 USD Received 10 Oct 2012; accepted 1 Nov 2012; published 20 Nov 2012